

FIRST EVIDENCE FOR SPECTRAL STATE TRANSITIONS IN THE ESO 243-49 HYPERLUMINOUS X-RAY SOURCE HLX-1

O. GODET¹, D. BARRET¹, N. A. WEBB¹, S. A. FARRELL², AND N. GEHRELS³

¹ Université de Toulouse, UPS, CESR, 9 Avenue du Colonel Roche, F-31028 Toulouse Cedex 9, France

² Department of Physics and Astronomy, University of Leicester, University Road, Leicester, LE1 7RH, UK

³ NASA/Goddard Space Flight Center, Greenbelt, MD 20771, USA

Received 2009 August 24; accepted 2009 September 23; published 2009 October 20

ABSTRACT

The brightest ultra-luminous X-ray source, ESO 243-49 HLX-1, with a 0.2–10 keV X-ray luminosity of up to 10^{42} erg s $^{-1}$, provides the strongest evidence to date for the existence of intermediate mass black holes (BHs). Although small-scale X-ray spectral variability has already been demonstrated, we have initiated a monitoring campaign with the X-ray Telescope (XRT) onboard the *Swift* satellite to search for luminosity-related spectral changes and to compare its behavior with the better-studied stellar mass BHs. In this Letter, we report a drop in the XRT count rate by a factor of ~ 8 which occurred simultaneously with a hardening of the X-ray spectrum. A second observation found that the source had re-brightened by a factor of ~ 21 which occurred simultaneously with a softening of the X-ray spectrum. This may be the first evidence for a transition between the low/hard and high/soft states.

Key words: accretion, accretion disks – X-rays: binaries – X-rays: individual (HLX-1)

1. INTRODUCTION

The most compelling evidence for the existence of intermediate mass black holes (IMBHs) comes from the observation of ultra-luminous X-ray sources (ULXs), extragalactic X-ray sources with bolometric luminosities exceeding 10^{39} erg s $^{-1}$ which are located outside the nucleus of the host galaxy. These X-ray luminosities—if they are assumed to be isotropically radiated—are up to several orders of magnitude above the Eddington limit for the maximum mass of stellar mass black holes (BHs; e.g., Roberts 2007). There is still an open debate about whether any ULXs host IMBHs. How IMBHs form and evolve is also a subject of intense debate, but they are thought to be associated with events such as the implosion of massive stars formed during the very first stages of star formation, the collapse of dense star clusters, and the early growth of supermassive BHs lying in the center of galaxies (Miller & Colbert 2004).

2XMM J011028.1-460421, referred to hereafter as HLX-1, was discovered serendipitously by *XMM-Newton* on 2004 November 23 (hereafter XMM1) in the outskirts of the edge-on spiral galaxy ESO 243-49, at a redshift of 0.0224 (Afonso et al. 2005). Its 0.2–10 keV unabsorbed X-ray luminosity, assuming isotropic emission, was found to be 1.1×10^{42} erg s $^{-1}$: 1 order of magnitude larger than the previously known brightest ULX (Miniutti et al. 2006). A second *XMM-Newton* observation performed four years later (on 2008 November 28—hereafter XMM2) revealed that the source spectrum and X-ray luminosity had changed. From its highest X-ray luminosity and the conservative assumption that the observed value exceeded the Eddington limit by a factor of 10, a lower limit of $500 M_{\odot}$ was derived for the BH in HLX-1, thus providing the strongest evidence so far that IMBHs do exist (Farrell et al. 2009).

The evidence for spectral variability in HLX-1 from the two *XMM-Newton* observations was the motivation for monitoring the source with the *Swift* X-ray Telescope (XRT; Burrows et al. 2005). The aim of this program is to study its spectral properties as a function of its X-ray luminosity to search for any of the three canonical X-ray states identified in Galactic black hole binaries (GBHBs; see, for instance, Remillard & McClintock 2006). Observing transitions between these states could thus

provide important information on the physical nature of ULXs (e.g., Kajava & Poutanen 2009). Despite its lower effective area compared to *XMM-Newton* and *Chandra*, the XRT can record enough counts in relatively short exposure times (few to tens of kiloseconds) to track any significant luminosity and spectral changes. This has been recently demonstrated by Kaaret & Feng (2009) who reported on a monitoring campaign with the XRT of three prototype ULXs, i.e., Holmberg IX X-1, NGC 5408 X-1, and NGC 4395 X-2. No spectral state changes were observed in any of these three sources, despite significant changes in their X-ray luminosities (by up to a factor of 9).

In this Letter, we present the results of the first two observations of our ongoing monitoring campaign of HLX-1 with the *Swift* XRT. Compared with a previous XRT pointing performed one year before, this observation revealed not only a dramatic drop in the XRT count rate (by a factor of ~ 8) but also a significant hardening of the X-ray spectrum as well as a dramatic re-brightening (by a factor ~ 21) occurring simultaneously with a clear softening of the X-ray spectrum.

2. X-RAY OBSERVATIONS

HLX-1 was observed with *Swift* under the Target-of-Opportunity (ToO) program on three occasions so far: S1 = 2008 October 24 (33.5 ks), S2 = 2009 August 5 (19.2 ks), and S3 = 2009 August 16 (19.1 ks). All the *Swift*-XRT Photon Counting data were processed using the tool XRTPipeline v0.12.3.⁴ We used the grade 0–12 events, giving slightly higher effective area at higher energies than the grade 0 events, and a 20 pixel (47.2 arcsec) radius circle to extract the source and background spectra using XSELECT v2.4a. The background extraction region chosen close to the source extraction region is the same for the three epochs S1, S2, and S3. No *XMM-Newton* sources are present inside the background extraction region. The average background count rate is $6.2 \pm 2.2 \times 10^{-4}$ counts s $^{-1}$. The ancillary response files were created using XRTMKARF v0.5.6 and exposure maps generated by XRTEXPOMAP v0.2.5.

⁴ See <http://heasarc.gsfc.nasa.gov/docs/swift/analysis/>.

Table 1
Summary of the X-ray Spectral Parameters for the Best Model Fits

Observation Number	Observation ^a Starting Date	Model	Spectral Parameters	L_X ^b (0.2–10 keV) ($\times 10^{41}$ erg s $^{-1}$)	χ^2/dof
S1	2008 Oct 24	ABS PL ^c	$\Gamma = 3.4 \pm 0.2$ $N_H^d = N_H^{\text{XMM2}}$	9.9 ± 0.5	20/16
S3	2009 Aug 16	ABS DBB ^c	$kT = 0.26 \pm 0.02$ keV $N_H^d = N_H^{\text{XMM2}}$	11.0 ± 1.0	14.4/21

Notes.

^a The S1 observation was performed between two *XMM-Newton* observations: XMM1 = 2004 Nov 23 and XMM2 = 2008 Nov 28.

^b The unabsorbed 0.2–10 keV luminosity was computed assuming a source distance of 95.5 Mpc and using the *WMAP* cosmology.

^c ABS PL: absorbed power-law; ABS DBB: absorbed disk blackbody.

^d $N_H^{\text{XMM2}} = 4 \times 10^{20}$ cm $^{-2}$ is the best constraint on N_H we derived from the XMM2 data (Farrell et al. 2009). It is the sum of the Galactic column absorption in the direction of HLX-1 $N_H^{\text{Gal}} = 2 \times 10^{20}$ cm $^{-2}$ (Dickey & Lockman 1990) and the intrinsic column absorption along the line of sight.

We fitted all the spectra within XSPEC v12.5.0a using the response file SWXPC0TO12S6_20070901V011.RMF, which includes an improvement of the soft energy response of the XRT (Godet et al. 2009a, 2009b) essential for a source as soft as HLX-1.

The XRT monitoring revealed that HLX-1 was highly variable over the past ten months, with a drop in count rate by a factor of ~ 8 from S1 to S2 followed by a dramatic re-brightening by a factor of ~ 21 from S2 to S3 (see Table 1).

Figure 1 shows the unfolded spectra for S1 (black), S2 (green), and S3 (red). The S1 and S3 spectra were binned to contain a minimum of 20 counts per channel, and were fitted using the χ^2 minimization technique. For all spectra, we fixed the absorption column at 4×10^{20} cm $^{-2}$, the best constraint on N_H derived by Farrell et al. (2009). All the best-fit models and spectral parameters are given in Table 1. From Figure 1, it is immediately obvious that the source has varied significantly in flux. The results from S1 when fitted using an absorbed power-law appear to be consistent with those of XMM1 (Farrell et al. 2009) which showed a steep power law, but are inconsistent with those of XMM2 ($\chi^2/\text{dof} = 134/18$ using the XMM2 best-fit model) even though the two observations were performed only a month apart. The addition of a disk blackbody (DBB) component to the power-law model does not significantly improve the fit ($\Delta\chi^2/\text{dof} = 3.1/2$; which corresponds to an *F*-test probability of 30%). The use of a unique absorbed DBB does not give a good fit either ($\chi^2/\text{dof} = 40.7/16$). The S3 spectrum is extremely soft. Within the statistics of the XRT data, the S3 spectrum is better fitted ($\chi^2/\text{dof} = 14.4/21$) using a unique absorbed soft thermal emission than an absorbed power law ($\chi^2/\text{dof} = 55.4/21$) with an N_H -value fixed at 4×10^{20} cm $^{-2}$. The sparse counts in S2 (28 counts in the background-subtracted spectrum) prevent us from performing any meaningful fitting analysis. Instead, we prefer to use spectral hardness ratios (see below). Nevertheless, folding through the *Swift*-XRT response kernel, the S1, XMM2, and S3 best-fit models multiplied by a constant factor give adequate fits to the S2 data with a constant factor of $\sim 8.2 \times 10^{-2}$ ($L \sim 8.1 \times 10^{40}$ erg s $^{-1}$) for S1, $\sim 8.3 \times 10^{-2}$ ($L \sim 5.0 \times 10^{40}$ erg s $^{-1}$) for XMM2, and $\sim 3.1 \times 10^{-2}$ ($L \sim 3.4 \times 10^{40}$ erg s $^{-1}$) for S3. The numbers in parentheses are the corresponding unabsorbed 0.2–10 keV luminosity. In all cases, the S2 luminosity appears to be much lower than those derived for XMM1, XMM2, S1, and S3 by at least a factor of 10. For comparison, we plot in Figure 1 the S2 spectrum (green) using a power law with a fixed value of the photon index $\Gamma = 2$.

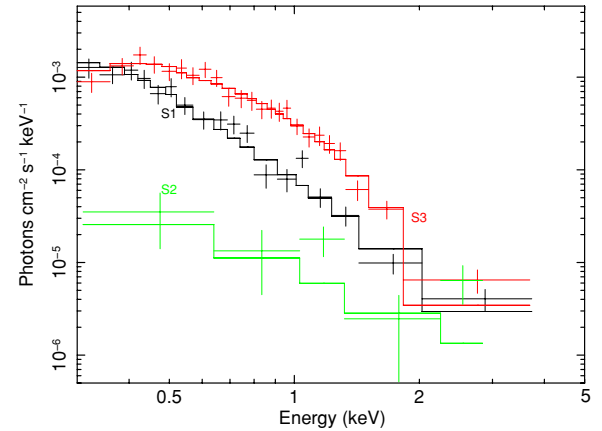


Figure 1. *Swift*-XRT PC grade 0–12 unfolded spectra of HLX-1: S1 (black) and S3 (red). The solid lines correspond to the best-fit models (see Table 1). For comparison, we plot the S2 spectrum (green) using a power law with a fixed value of the photon index $\Gamma = 2$. We used the XSPEC command SETPLOT REBIN 7 7 to improve the visual aspect of the S2 spectrum.

The fitting results are suggestive of a series of spectral changes. To investigate this, we compared the total number of counts in three energy bands: 0.3–1 keV, 1–3 keV, and 3–10 keV (see Table 2). There is a significant drop (by a factor of ~ 16) in the soft 0.3–1 keV band between S1 and S2 when compared to the 1–3 keV band. This suggests a hardening of the spectrum between S1 and S2. The source was not detected above 3 keV in either the S2 or S3 data due to an overall low flux level in S2 and a steep spectral slope in S3. From S2 to S3, there is a significant increase in counts (by a factor of ~ 44) in the 0.3–1 keV band when compared to the other bands, indicating that the X-ray spectrum has softened again (see also Table 1).

3. STATE TRANSITIONS IN A ULX?

The detection of the same spectral states as those observed in the GBHBs would be extremely valuable in constraining the nature of ULXs. Spectra of other ULXs have been interpreted either as the source being in a low/hard state or in a very high state, even if the distinction between the two states is problematic (e.g., Soria & Kuncic 2008). It appears that ULXs in the high/soft or thermal state are rare. Thermal components with temperatures in the range $kT = 1$ –1.5 keV have been observed in the spectra of some ULXs for an emitted luminosity $L_X < 10^{39}$ erg s $^{-1}$, placing them at the extreme end of stellar mass BHs (Roberts et al. 2002). Winter et al. (2006) claimed

Table 2
Comparison of the Number of Counts in Three Energy Bands: 0.3–1 keV, 1–3 keV, and 3–10 keV

Observation Number	Exposure Time (ks)	Counts ^a (0.3–1 keV)	Counts ^a (1–3 keV)	Counts ^a (3–10 keV)	Count rate (0.3–10 keV) (counts s ⁻¹)
S1	33.45 (19.17)	274 ± 17 (157 ± 13) ^b	97 ± 10 (56 ± 7) ^b	18 ± 5 (10 ± 4) ^b	1.2×10^{-2}
S2	19.17	10 ± 4	18 ± 5	0^{+2}_{-0}	1.5×10^{-3}
S3	19.09 (19.17)	437 ± 21 (438 ± 21) ^b	185 ± 14 (186 ± 14) ^b	0^{+2}_{-0}	3.3×10^{-2}

Notes. The last column gives the source count rate in the 0.3–10 keV band. All the numbers were derived using a 20 pixel radius circle for the source and the background.

^a The errors quoted above are 1σ error. When the number of counts in a given energy band is less than 20, the 1σ errors were computed using the following formula: $\sigma = 1 + \sqrt{N} + 0.75$ instead of $\sigma = \sqrt{N}$ (Gehrels et al. 1986).

^b The number of counts are computed using an exposure time of 19.17 ks to facilitate the comparison between all the *Swift* observations.

the identification of several ULXs in the thermal state based on the detection of DBB spectral components. However, in all cases, the DBB contribution was not significant with respect to the power-law component. Moreover, no state transition as seen in GBHBs has been observed in ULXs even those showing large luminosity variability (e.g., Gladstone & Roberts 2009; Fridriksson et al. 2008). Claims for spectral state transitions, different from those seen in GBHBs, have already been reported (see, e.g., Liu et al. 2002; Soria & Motch 2004). In these papers, the authors claimed evidence for a high/hard to low/soft transition. Recently, Isobe et al. (2009) claimed evidence for a spectral transition in the ULX, NGC 2403 Source 3 from a slim-disk state dominated by a ~ 1 keV DBB to a very high state dominated by a power-law spectrum.

When compared to other ULXs, HLX-1 is truly remarkable not only because its huge luminosity enables us to claim that it may harbor an IMBH with a $> 500 M_{\odot}$ mass (Farrell et al. 2009), but also because its luminosity-spectral variability as observed in X-rays (see Section 2) shows compelling evidence for spectral variation on short timescales (see Figure 2) that are consistent with what has been observed in GBHBs like GRS 1915+105 (Fender & Belloni 2004). Indeed, HLX-1 was likely to be in the very high state in XMM1 and S1, while the source was in the high/soft state in XMM2 with a DBB luminosity corresponding to 80% of the total X-ray luminosity. In this case, the transition has occurred in a one month window. In S2, the data suggest that the source may have been in the low/hard state. The re-brightening and spectral softening in S3 suggest that HLX-1 has returned to a high/soft state brighter than during XMM2, the transition having occurred on a relatively short timescale (< 7 days).

The low temperature of the DBB component measured in XMM2 and S3 is in the same range as those measured in some ULXs (~ 0.1 –0.2 keV; see Soria & Kuncic 2008). This thermal component is often interpreted as direct emission from the accretion disk. The DBB normalization K (XMM2) ~ 29 and K (S3) ~ 14.3 (via the inner radius of the accretion disk R_{in}) could then be used to constrain the BH mass. To do so, we assumed that R_{in} corresponds to the radius of the last stable orbit around a non-rotating BH or a rotating BH with a maximum angular momentum (i.e., $R_{\text{in}} = 0.5$ – $3R_S \sim 1.5$ – 9 km ($\frac{M}{M_{\odot}}$)) with $R_S = \frac{2GM}{c^2}$, the Schwarzschild radius where M , c , and G are the BH mass, the speed of light, and the gravitational constant, respectively). We found that the derived masses are in the range of IMBH masses with $M \sim 5.7 \times 10^3$ – $3.4 \times 10^4 M_{\odot}(\cos(\theta))^{-\frac{1}{2}}$

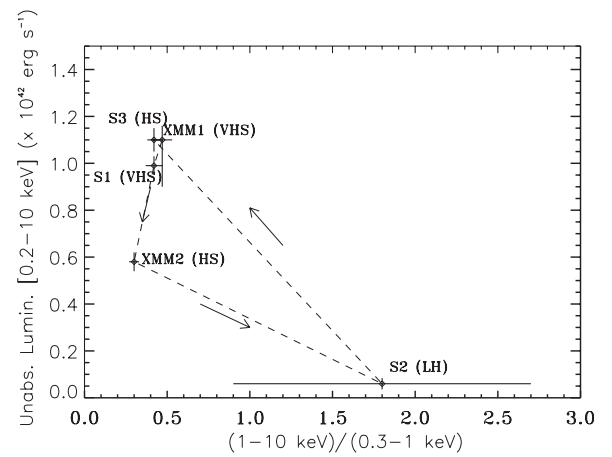


Figure 2. Hardness intensity diagram using the *Swift* and *XMM-Newton* data. The XMM1 and XMM2 points were computed by convolving with the XRT spectral response the best-fit models in XMM1 and XMM2, respectively. All the errors are 1σ errors. The S2 0.2–10 keV unabsorbed luminosity was derived by folding through the *Swift*-XRT response kernel the S1, XMM2, and S3 best-fit models multiplied by a constant factor (see Section 2) and taking the lowest ($L \sim 3.4 \times 10^{40}$ erg s⁻¹) and highest ($L \sim 8.1 \times 10^{40}$ erg s⁻¹) values.

from XMM2 and $M \sim 4 \times 10^3$ – $2.4 \times 10^4 M_{\odot}(\cos(\theta))^{-\frac{1}{2}}$ from S3, where θ is the inclination of the disk with respect to the line of sight.

Within the limited statistics of the XRT spectrum, we have attempted to fit the highest quality spectrum (S3) with the slim-disk model (Kawaguchi 2003). In order to reduce the number of free parameters, we froze the source distance to 95 Mpc and the viscosity parameter to three possible values (0.01, 0.1, and 1). The fits suggest a BH mass larger than $10^3 M_{\odot}$, thus adding another piece of evidence for the presence of an IMBH in HLX-1.

4. CONCLUSION

We have presented the first evidence for spectral state transitions in HLX-1, similar to those seen in GBHBs, strengthening the case for a BH in the system. Since multi-wavelength observations (e.g., IR, radio) of HLX-1 continue to exclude alternative explanations for HLX-1, such as a foreground neutron star or a background narrow line Seyfert 1 galaxy (N. A. Webb et al. 2009, in preparation), HLX-1 still provides the strongest evidence for the existence of IMBHs in the universe.

O.G. acknowledges funding from the CNRS and the CNES. S.A.F. acknowledges STFC funding. We also thank Cole Miller for useful discussions.

Facilities: *XMM-Newton, Swift*

REFERENCES

- Afonso, J., et al. 2005, *ApJ*, **624**, 135
 Burrows, D. N., et al. 2005, *Space Sci. Rev.*, **120**, 165
 Dickey, J. M., & Lockman, F. J. 1990, *ARA&A*, **28**, 215
 Farrell, S. A., Webb, N. A., Barret, D., Godet, O., & Rodrigues, J. M. 2009, *Nature*, **460**, 73
 Fender, R., & Belloni, T. 2004, *ARA&A*, **42**, 317
 Fridriksson, J. K., Homan, J., Lewin, W. H. G., Kong, A. K. H., & Pooley, D. 2008, *ApJS*, **177**, 465
 Gehrels, N. 1986, *ApJ*, **303**, 336
 Gladstone, J. C., & Roberts, T. P. 2009, *MNRAS*, **397**, 124
 Godet, O., et al. 2009a, Release Note on the *Swift*-XRT Spectral Response SWIFT-XRT-CALDB-13
 Godet, O., et al. 2009b, *A&A*, **494**, 775
 Isobe, N., et al. 2009, *PASJ*, **61**, 279
 Kaaret, P., & Feng, H. 2009, *ApJ*, **702**, 1679
 Kajava, J. J. E., & Poutanen, J. 2009, *MNRAS*, **398**, 1450
 Kawaguchi, T. 2003, *ApJ*, **593**, 69
 Liu, J.-F., et al. 2002, *ApJ*, **581**, L93
 Miller, M. C., & Colbert, E. J. M. 2004, *Int. J. Modern Phys. D*, **13**, 1
 Miniutti, G., et al. 2006, *MNRAS*, **373**, 1
 Remillard, R. A., & McClintok, J. E. 2006, *ARA&A*, **44**, 49
 Roberts, T. P. 2007, *Ap&SS*, **311**, 203
 Roberts, T. P., Warwick, R. S., Ward, J. M., & Murray, S. S. 2002, *MNRAS*, **337**, 677
 Soria, R., & Kuncic, Z. 2008, in AIP Conf. Proc. 1053, Proc. 2nd Kolkata Conference on Observational Evidence for Black Holes in the Universe, ed. S. K. Chakrabarti & A. S. Majumdar (Melville, NY: AIP), **103**
 Soria, R., & Motch, C. 2004, *A&A*, **422**, 915
 Winter, L. M., Mushotzky, R. F., & Reynolds, C. S. 2006, *ApJ*, **649**, 730